



Synthesis of Li₂S-Carbon Cathode Materials via Carbothermic Reduction of Li₂SO₄

Jiayan Shi¹, Jian Zhang², Yifan Zhao², Zheng Yan¹, Noam Hart¹ and Juchen Guo^{1,2*}

¹ Department of Chemical and Environmental Engineering, University of California, Riverside, Riverside, CA, United States,

² Materials Science and Engineering Program, University of California, Riverside, Riverside, CA, United States

Pre-lithiated sulfur materials are promising cathode for lithium-sulfur batteries. The synthesis of lithium sulfide-carbon (Li₂S-C) composite by carbothermic reduction of lithium sulfate (Li₂SO₄) is investigated in this study. The relationship between reaction temperature and the consumption of carbon in the carbothermic reduction of Li₂SO₄ is first investigated to precisely control the carbon content in the resultant Li₂S-C composites. To understand the relationship between the material structure and the electrochemical properties, Li₂S-C composites with the same carbon content are subsequently synthesized by controlling the mass ratio of Li₂SO₄/carbon and the reaction temperature. Systematic electrochemical analyses and microscopic characterizations demonstrate that the size of the Li₂S particles dispersed in the carbon matrix is the key parameter determining the electrochemical performance. A reversible capacity of 600 mAh g⁻¹ is achieved under lean electrolyte condition with high Li₂S areal loading.

Keywords: lithium-sulfur batteries, lithium sulfide, lithium sulfate, carbothermic reaction, carbon composite

OPEN ACCESS

Edited by:

Wen Liu,
Beijing University of Chemical
Technology, China

Reviewed by:

Huan Pang,
Yangzhou University, China
Xifei Li,
Xi'an University of Technology, China

*Correspondence:

Juchen Guo
jguo@enrg.ucr.edu

Specialty section:

This article was submitted to
Electrochemical Energy Conversion
and Storage,
a section of the journal
Frontiers in Energy Research

Received: 02 March 2019

Accepted: 16 May 2019

Published: 04 June 2019

Citation:

Shi J, Zhang J, Zhao Y, Yan Z, Hart N
and Guo J (2019) Synthesis of
Li₂S-Carbon Cathode Materials via
Carbothermic Reduction of Li₂SO₄.
Front. Energy Res. 7:53.
doi: 10.3389/fenrg.2019.00053

INTRODUCTION

Lithium-sulfur (Li-S) batteries have received intensive investigations over the past decade due to its great potential as a high-capacity rechargeable battery technology (Ma et al., 2015; Manthiram et al., 2015; Wild et al., 2015; Fang et al., 2017; Peng et al., 2017; Zheng et al., 2017; Chen et al., 2018). To eliminate the potential safety hazard induced by the Li metal anode, high-capacity non-Li anodes, particularly silicon-based materials, have been sought as the alternative (Yang et al., 2010; Agostini et al., 2014; Cao et al., 2015; Jha et al., 2015; Guo et al., 2017). Utilizing non-Li anodes requires lithium sulfide (Li₂S) cathode materials, which have been produced by a number of methods reported in literature. The most common method is to physically mix Li₂S and carbon materials with high-energy ball milling (Cai et al., 2012; Jeong et al., 2013; Chen et al., 2014; Liu et al., 2015a; Lee et al., 2016; Liang et al., 2016). Li₂S solution in ethanol was used to deposit Li₂S on various carbon structures (Wu et al., 2014a,b,c, 2015, 2016; Wang et al., 2015; Han et al., 2016; Zhou et al., 2016). Other solvent such as anhydrous methyl acetate was also used to disperse Li₂S in carbon (Seh et al., 2014). A number of chemical methods were also reported: Li₂S-C composite could be produced from sulfurization of lithium carbonate with H₂S (Dressel et al., 2016; Hart et al., 2018). Li₂S-C composite was also synthesized via the reaction between lithium polysulfides and the nitrile group in polyacrylonitrile (Guo et al., 2013). A recently reported novel method utilized the thermal reaction between metallic Li and gaseous carbon disulfide (CS₂) to form carbon coated Li₂S in one step (Tan et al., 2017). Another chemical method to produce Li₂S-C composites is to

TABLE 1 | Elemental analysis of KJB before and after the hydrogen reduction treatment.

Elements	C (wt.%)	H (wt.%)	N (wt.%)	O (wt.%)
Before	97.72	0.48	0.29	1.51
After	98.87	0.22	0.17	0.74

convert lithium sulfate (Li_2SO_4) to Li_2S via carbothermic reduction (Yang et al., 2013; Kohl et al., 2015; Li et al., 2015; Liu et al., 2015b; Wang et al., 2016; Yu et al., 2017; Zhang et al., 2017; Ye et al., 2018). Comparing to all other methods mentioned above, carbothermic reduction of Li_2SO_4 involves neither hazardous gas such as gaseous CS_2 or H_2S , nor air sensitive reactants such as Li_2S or Li metal. Furthermore, $\text{Li}_2\text{S-C}$ composites can be produced in one-step reaction in carbothermic reduction of Li_2SO_4 . In this study, we focus on understanding the effect of reaction temperature on stoichiometric ratio of $\text{C}/\text{Li}_2\text{SO}_4$ in the carbothermic reduction and the structure-property relationship of the obtained $\text{Li}_2\text{S-C}$ composites as the cathode materials for Li-S batteries.

MATERIALS AND METHODS

Temperature Effect on $\text{C}/\text{Li}_2\text{SO}_4$ Stoichiometric Ratio

All reagents were used after purchase without further purification unless otherwise noted. Ketjen black EC-600JD (KJB, purchased from AkzoNobel) was used as the carbon source in this study. To minimize the effect of the impurity in KJB (mainly oxygen) on the carbothermic reduction of Li_2SO_4 , KJB was treated by hydrogen reduction: In a typical experiment, approximately 400 mg KJB was heated under hydrogen/argon (5%/95%) environment at $1,000^\circ\text{C}$ for 3 h. Elemental contents of KJB before and after the hydrogen treatment was analyzed as shown in **Table 1**.

Li_2SO_4 and KJB was thoroughly mixed by mechanical ball milling with different weight ratios including 2.0:1, 2.3:1, 2.5:1 and 2.9:1. The mixture was heated in a tube furnace under flowing argon (Ar) environment to form $\text{Li}_2\text{S-C}$ composite. The temperature of the tube furnace was first raised to 200°C from room temperature at 5°C min^{-1} . The temperature was held at 200°C for 2 h, followed by further increasing to either 700 or 750°C at 5°C min^{-1} . The temperature was kept at 700 or 750°C for 6 h to complete the carbothermic reduction of Li_2SO_4 . Ethanol was used to leach out the Li_2S in the resultant $\text{Li}_2\text{S-C}$ composite to measure the conversion of Li_2SO_4 and carbon content, from which the $\text{C}/\text{Li}_2\text{SO}_4$ stoichiometric ratio in the carbothermic reduction can be calculated.

$\text{Li}_2\text{S-C}$ Composite Synthesis and Characterization

To improve the areal loading the $\text{Li}_2\text{S-C}$ composite at the cathode, micron-sized carbon particles were first synthesized with KJB as the precursor following the method reported by Lv et al. (2015). In a typical synthesis of $\text{Li}_2\text{S-C}$ composite, the micron-sized carbon particles were mixed into 5 mL aqueous

solution of Li_2SO_4 with a specific $\text{Li}_2\text{SO}_4/\text{C}$ ratio, followed by dispersion by sonication for 5 min and thorough stir for additional 24 h. One hundred milliliter ethanol was then added into the mixture and stirred for 10 min. The $\text{Li}_2\text{SO}_4\text{-C}$ dispersion in the water/ethanol mixture was dried with rotary evaporator at 90°C . The obtained $\text{Li}_2\text{SO}_4\text{-C}$ mixture was further dried at 80°C under vacuum overnight. To produce the $\text{Li}_2\text{S-C}$ composite, 0.5 g of $\text{Li}_2\text{SO}_4\text{-C}$ mixture was heated under flowing Ar environment in a tube furnace using the same process as aforementioned.

The $\text{Li}_2\text{S-C}$ composite was characterized by powder X-Ray diffraction (XRD, PANalytical). Kapton tape was used to seal the XRD sample to prevent Li_2S from reacting with moisture in the ambient environment. Nitrogen adsorption-desorption isotherms of the $\text{Li}_2\text{S-C}$ composites were measured with a surface area and porosity analyzer (Micromeritics ASAP2020). The surface area was obtained with the Brunauer-Emmett-Teller (BET) method. To avoid Li_2S reacting with environmental moisture, all $\text{Li}_2\text{S-C}$ composites were transferred into the BET sample tube in the glovebox and sealed with Teflon tape. The microstructure of the $\text{Li}_2\text{S-C}$ composites was characterized with scanning electron microscopy (SEM) and elemental mapping was obtained by energy-dispersive X-ray spectroscopy (EDX). To perform the SEM characterization, the samples were carefully sealed into a stainless-steel vacuum tube in an Ar-filled glovebox. The sample tube was transferred into the SEM chamber under flowing argon protection using a glove-bag.

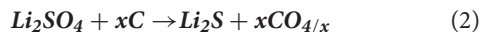
Electrode Fabrication, Cell Assembly and Testing

To prepare the electrode, $\text{Li}_2\text{S-C}$ composite was mixed with carbon black and polyvinylidene difluoride with a weight ratio of 85:5:10 in N-methyl-2-pyrrolidone. The obtained slurry was uniformly pasted on a carbon coated aluminum foil current collector and dried in the Ar-filled glovebox at 135°C for at least 15 h. The dried electrodes were assembled into 2032-type coin cells with Li foil anode (99.9%, Alfa Aesar) and Celgard[®] 2500 separator. The electrolyte used in this study was 1 M lithium bis(trifluoromethanesulfonyl)imide solution in a mixture of 1,3-dioxolane, dimethoxyethane and 1-butyl-1-methylpyrrolidinium bis(trifluoromethanesulfonyl)imide (1:1:2 by vol.) with 1.5 wt.% of LiNO_3 . The electrolyte to Li_2S ratio ($\mu\text{L}/\text{mg}$) was kept at 7 in all coin cells testing. The average areal loading of Li_2S on the electrode is 2 mg cm^{-2} . The first charge (activation) was performed at a rate of $\text{C}/50$ (24 mA g^{-1}) to a charge cutoff of 3.8 V vs. Li^+/Li . The subsequent cycles were performed at $\text{C}/10$, $\text{C}/5$, $\text{C}/2$, and 1C between 2.8 and 1.7 V.

RESULTS AND DISCUSSION

Despite the previous reports on synthesizing $\text{Li}_2\text{S-C}$ composites via carbothermic reduction of Li_2SO_4 , the influence of reaction temperature on the stoichiometric ratio between carbon and Li_2SO_4 has not been investigated. As shown in **Reaction 1**, carbothermic reduction of Li_2SO_4 generally produces both carbon dioxide (CO_2) and carbon monoxide (CO) (Li et al., 2015; Zhang et al., 2017). However, the ratio between CO_2 and

CO changes with temperature due to their different stability as the function of temperature (Zhang et al., 2017). Therefore, the carbothermic reduction of Li_2SO_4 can be expressed as **Reaction 2**, in which the stoichiometric ratio of $\text{C}/\text{Li}_2\text{SO}_4$, x , is a function of temperature. To synthesize $\text{Li}_2\text{S-C}$ composite in one-step carbothermic reduction with precise carbon content, it is critical to learn the value of x at different temperature.

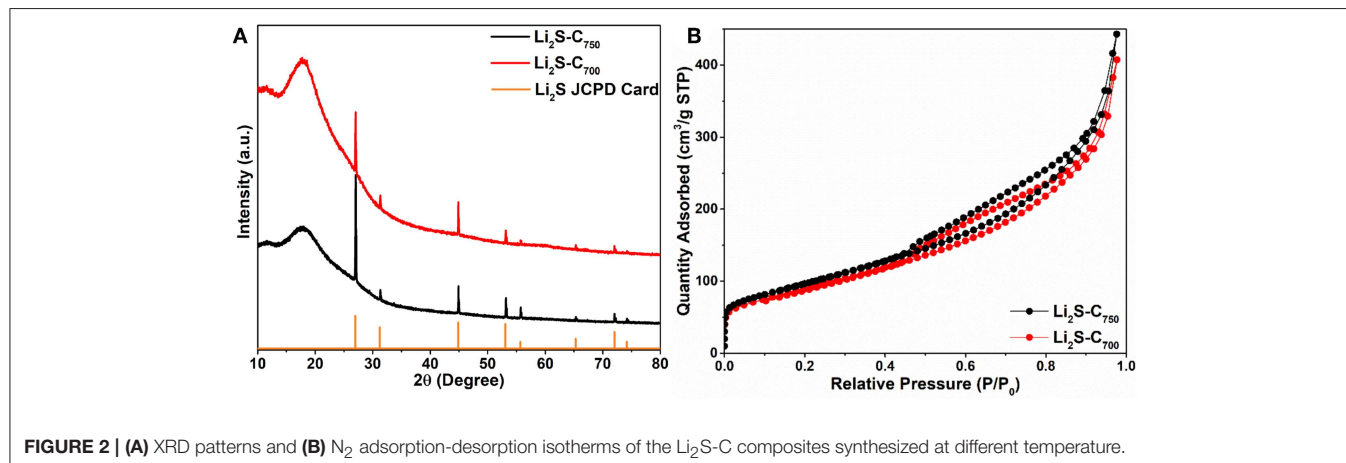
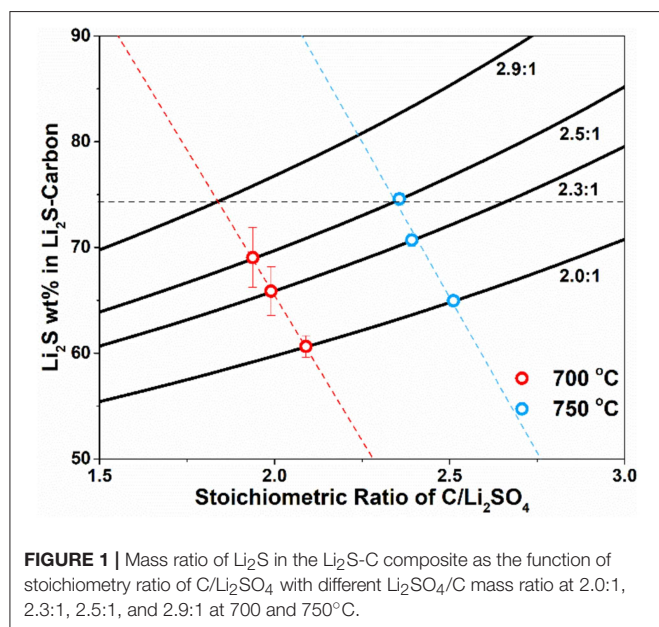


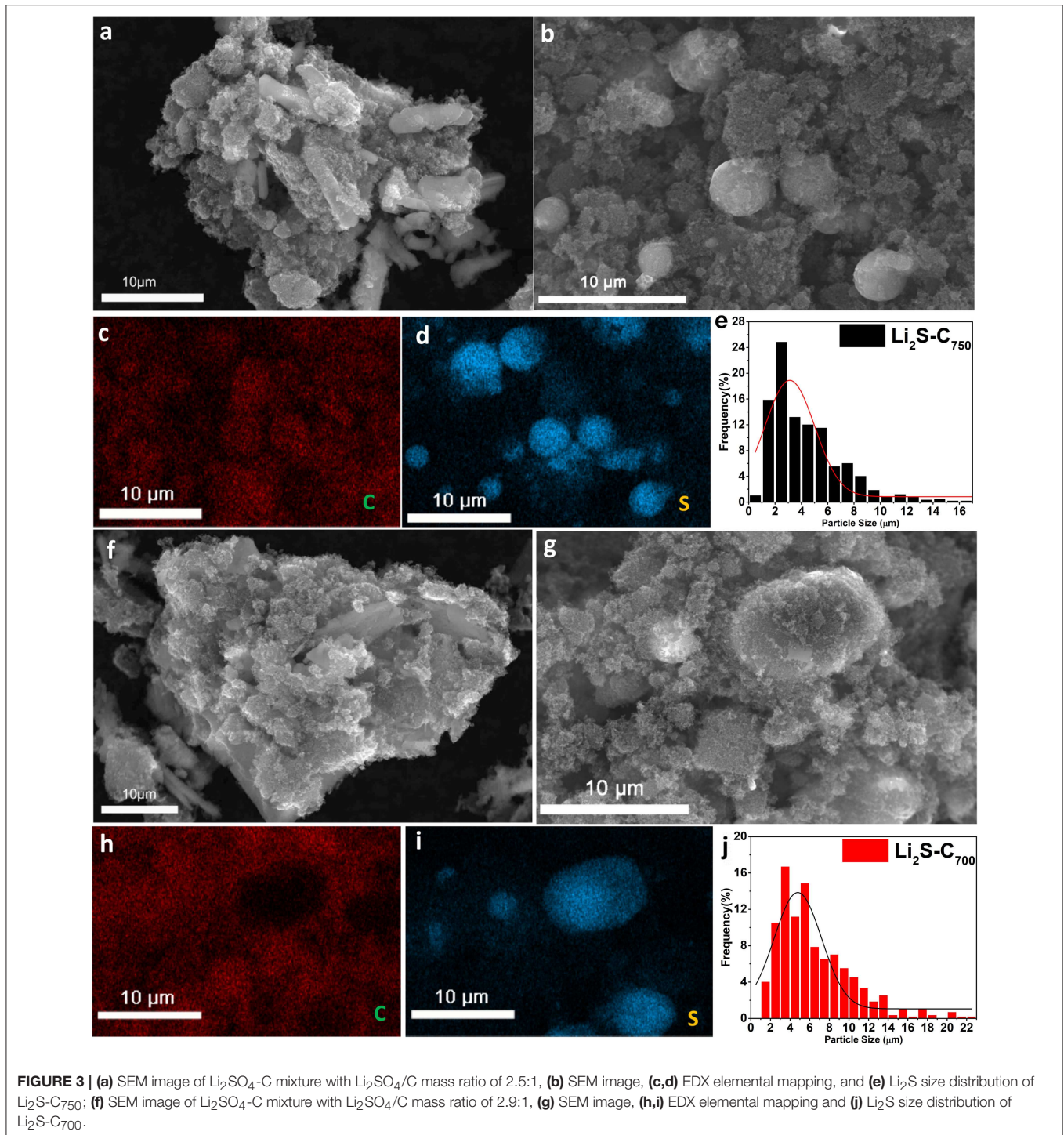
With certain $\text{Li}_2\text{SO}_4/\text{C}$ mass ratio (carbon in excess) and assumption of 100% conversion of Li_2SO_4 to Li_2S , the Li_2S content in the $\text{Li}_2\text{S-C}$ composite from the carbothermic reduction can be calculated as the function of the stoichiometric ratio of $\text{C}/\text{Li}_2\text{SO}_4$ as shown in **Figure 1**. The four solid lines represent four different $\text{Li}_2\text{SO}_4/\text{C}$ mass ratio, 2.0:1, 2.3:1, 2.5:1,

and 2.9:1, which all have excess of carbon. Carbothermic experiments were first performed with $\text{Li}_2\text{SO}_4/\text{C}$ mass ratio of 2.0:1, 2.3:1 and 2.5:1 at 700 and 750°C. The reaction at each condition (temperature and $\text{Li}_2\text{SO}_4/\text{C}$ mass ratio) was repeated at least three times to minimize experimental errors. The content of Li_2S in the resultant $\text{Li}_2\text{S-C}$ composite was measured and the results demonstrated full conversion of Li_2SO_4 to Li_2S in all experiments. Therefore, the stoichiometric ratio of $\text{C}/\text{Li}_2\text{SO}_4$, x , was calculated at all experimental conditions and the average values were marked on the theoretic curves in **Figure 1**. It is clear that the stoichiometric ratio of $\text{C}/\text{Li}_2\text{SO}_4$ is lower at 700°C, indicating less carbon is consumed at lower temperature with higher CO_2 content in the gaseous products. The experimental results can also be linearly fitted to obtain an empirical relationship between Li_2S content in $\text{Li}_2\text{S-C}$ and the stoichiometric $\text{C}/\text{Li}_2\text{SO}_4$ ratio at different temperature. The empirical relationship at 700°C is $\text{Li}_2\text{S wt.}\% = 175.3 - 54.9x$ (red dotted line) and the one at 750°C is $\text{Li}_2\text{S wt.}\% = 212.0 - 58.6x$ (blue dotted line).

To study the structure-property relationship of the $\text{Li}_2\text{S-C}$ composites, we need to select a composite from each reaction temperature with same Li_2S content. One selected $\text{Li}_2\text{S-C}$ composite is produced at 750°C with $\text{Li}_2\text{SO}_4/\text{C}$ mass ratio of 2.5:1, which contains 72 wt.% of Li_2S . The same Li_2S content was projected on the empirical linear fitting of Li_2S content vs. stoichiometric $\text{C}/\text{Li}_2\text{SO}_4$ ratio at 700°C, from which the required $\text{Li}_2\text{SO}_4/\text{C}$ mass ratio was calculated to be 2.9:1. The carbothermic reduction of Li_2SO_4 at 700°C with $\text{Li}_2\text{SO}_4/\text{C}$ mass ratio of 2.9:1 yielded $\text{Li}_2\text{S-C}$ with 71 wt.% Li_2S content, which agreed very well with the prediction.

The two $\text{Li}_2\text{S-C}$ composites with the same Li_2S content are denoted as $\text{Li}_2\text{S-C}_{700}$ and $\text{Li}_2\text{S-C}_{750}$ according to the reaction temperature. The XRD patterns of these two composites in **Figure 2A** indicate well-crystallized Li_2S formed from the carbothermic reduction of Li_2SO_4 . The broad peak around 20° is due to the Kapton tape protecting Li_2S from reacting to the ambient moisture. Based on the full-width at half-maximum of the XRD peaks, $\text{Li}_2\text{S-C}_{750}$ has smaller crystal grain size than that of $\text{Li}_2\text{S-C}_{700}$. The BET surface areas of these two

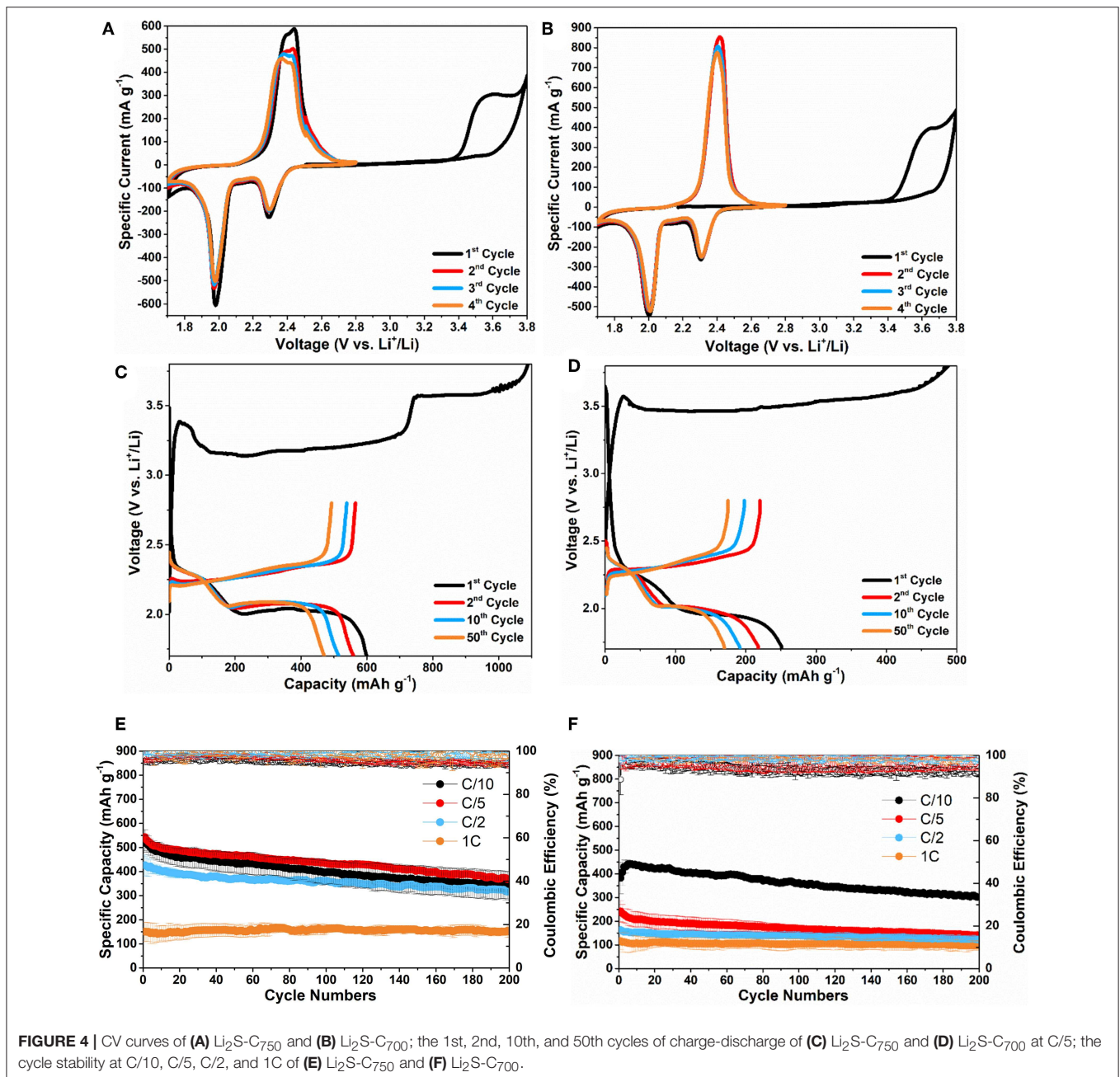




$\text{Li}_2\text{S-C}$ composites from the N_2 adsorption-desorption isotherms (Figure 2B) are very close: $350.8 \text{ m}^2 \text{ g}^{-1}$ for $\text{Li}_2\text{S-C}_{750}$ and $326.8 \text{ m}^2 \text{ g}^{-1}$ for $\text{Li}_2\text{S-C}_{700}$. We believe the higher carbon content in the $\text{Li}_2\text{SO}_4\text{-C}$ mixture at the 750°C reaction alleviated the particle aggregation thus leading to smaller Li_2S particles.

SEM was used to characterize the microstructure of the $\text{Li}_2\text{S-C}$ composites. Figure 3a shows the structure of the $\text{Li}_2\text{SO}_4/\text{C}$

mixture before carbothermic reduction for $\text{Li}_2\text{S-C}_{750}$. Li_2SO_4 exhibited typical monoclinic crystal structure as hexagonal plate with crystal size around $10 \mu\text{m}$. Interestingly, the carbothermic reduction of Li_2SO_4 yielded spherical Li_2S particles dispersed in carbon matrix as displayed in the SEM image in Figure 3b and the EDX elemental mapping in Figures 3c,d. The SEM characterization of the $\text{Li}_2\text{S-C}_{700}$ demonstrated very similar



microstructure with $\text{Li}_2\text{S-C}_{750}$ as displayed in **Figures 3f-i**. The particle size of Li_2S was measured by ImageJ software and the average particle size was analyzed by Gaussian distribution over 700 particles. As the particle size distribution shown in **Figures 3e,j**, the Li_2S particle size in $\text{Li}_2\text{S-C}_{750}$ was smaller than that in $\text{Li}_2\text{S-C}_{700}$: The average Li_2S particle size was 4.4 μm in $\text{Li}_2\text{S-C}_{750}$ and 6.4 μm in $\text{Li}_2\text{S-C}_{700}$.

Figures 4A,B show the CV cycles of $\text{Li}_2\text{S-C}_{750}$ and $\text{Li}_2\text{S-C}_{700}$ electrodes. The $\text{Li}_2\text{S-C}_{750}$ electrode demonstrated slightly lower delithiation potential than $\text{Li}_2\text{S-C}_{700}$ in the first cycle (3.5 vs. 3.6 V for the cathodic peak, respectively). This observation is consistent with the first galvanostatic delithiation (charge)

curves of these two composites shown in **Figures 4C,D**. $\text{Li}_2\text{S-C}_{750}$ clearly demonstrated a lower activation potential at approximately 3.2 V vs. Li^+/Li in the first two third of the charge process. On the contrary, $\text{Li}_2\text{S-C}_{700}$ showed much higher activation potential at 3.5 V vs. Li^+/Li , which led to a lower first charge capacity. We speculate that the lower delithiation overpotential of $\text{Li}_2\text{S-C}_{750}$ is attributed to its structural advantage, mainly smaller Li_2S particle size. Previous studies also reported that larger Li_2S particle size could result to higher activation potential in the first charge process (Yang et al., 2012; Kohl et al., 2015; Liu et al., 2015a; Wang et al., 2016; Ye et al., 2018). In addition to the effect from particle size, activation

potential of Li_2S can also be affected by surface impurities such as Li_2SO_4 , Li_2CO_3 , and Li_2O (Jung and Kang, 2016; Vizintin et al., 2017). The better microstructure of $\text{Li}_2\text{S-C}_{750}$ is also evidenced by the lower charge-discharge potential hysteresis (Figures 4C,D), better cycle stability and rate capability shown in Figures 4E,F. The average initial discharge capacity of $\text{Li}_2\text{S-C}_{750}$ is 600 mAh g^{-1} (average of 3 electrodes), and 400 mAh g^{-1} capacity was retained after 200 cycles at C/5. The specific capacity of $\text{Li}_2\text{S-C}_{750}$ at C/2 only slightly decreased from C/10 and C/5, indicating good rate capability. On the other hand, $\text{Li}_2\text{S-C}_{700}$ suffered from not only lower specific capacity at C/10, but also inferior rate capability as indicated by the low capacity at C/5, C/2, and 1C. It is clear that particle size of Li_2S is the critical parameter for rate performance of the $\text{Li}_2\text{S-C}$ composites. It is also worth noting that the initial specific capacity of $\text{Li}_2\text{S-C}_{700}$ started with slight increase during cycling at C/10, which can be attributed to its inferior activation process due to larger Li_2S particle size.

CONCLUSION

In summary, the synthetic route of $\text{Li}_2\text{S-C}$ from carbothermic reduction of Li_2SO_4 was investigated in this study. Particularly the relationship between reaction temperature and

stoichiometric ratio of $\text{C/Li}_2\text{SO}_4$ in the carbothermic reduction was obtained for the first time. Through investigations on microstructures and electrochemical properties, we speculated that smaller Li_2S particle size dispersed in carbon matrix is the key parameter to improve the electrochemical performance. Methods to further reduce particle size of Li_2S via carbothermic reduction of Li_2SO_4 will be investigated in future studies.

DATA AVAILABILITY

All datasets generated for this study are included in the manuscript and/or the supplementary files.

AUTHOR CONTRIBUTIONS

JS performed the majority of the experiments. JZ performed SEM and EDX. YZ and ZY synthesized the micron-sized carbon particles used in $\text{Li}_2\text{S-C}$ synthesis. NH and JG designed the experiments. All authors co-wrote the manuscript.

ACKNOWLEDGMENTS

We acknowledge the National Science Foundation for financial support under grant no. CBET-1604908.

REFERENCES

- Agostini, M., Hassoun, J., Liu, J., Jeong, M., Nara, H., Momma, T., et al. (2014). A lithium-ion sulfur battery based on a carbon-coated lithium-sulfide cathode and an electrodeposited silicon-based anode. *ACS Appl. Mater. Interfaces* 6, 10924–10928. doi: 10.1021/am4057166
- Cai, K., Song, M., Cairns, E., and Zhang, Y. (2012). Nanostructured $\text{Li}_2\text{S-C}$ composites as cathode material for high-energy lithium/sulfur batteries. *Nano Lett.* 12, 6474–6479. doi: 10.1021/nl303965a
- Cao, R., Xu, W., Lv, D., Xiao, J., and Zhang, J. (2015). Anodes for rechargeable lithium-sulfur batteries. *Adv. Energy Mater.* 5:1402273. doi: 10.1002/aenm.201402273
- Chen, L., Guo, X., Lu, W., Chen, M., Li, Q., Xue, H., et al. (2018). Manganese monoxide-based materials for advanced batteries. *Coordination Chem. Rev.* 368, 13–34. doi: 10.1016/j.ccr.2018.04.015
- Chen, L., Liu, Y., Ashuri, M., Liu, C., and Shaw, L. L. (2014). Li_2S encapsulated by nitrogen-doped carbon for lithium sulfur batteries. *J. Mater. Chem. A* 2:18026. doi: 10.1039/C4TA04103H
- Dressel, B. C., Jha, H., Eberle, A., Gasteiger, A. H., and Fassler, F. T. (2016). Electrochemical performance of lithium-sulfur batteries based on a sulfur cathode obtained by H_2S gas treatment of a lithium salt. *J. Power Sources* 307, 844–848. doi: 10.1016/j.jpowsour.2015.12.140
- Fang, R., Zhao, S., Sun, Z., Wang, D. W., Cheng, H. M., et al. (2017). More reliable lithium-sulfur batteries: status, solutions and prospects. *Adv. Mater.* 29:1606823. doi: 10.1002/adma.201606823
- Guo, J., Yang, Z., Yu, Y., Abruña, H. D., and Archer, L. A. (2013). Lithium-sulfur battery cathode enabled by lithium-nitrile interaction. *J. Am. Chem. Soc.* 135, 763–767. doi: 10.1021/ja309435f
- Guo, X., Zheng, S., Zhang, G., Xiao, X., Li, X., Xu, Y., et al. (2017). Nanostructured graphene-based materials for flexible energy storage. *Energy Storage Mater.* 9, 150–169. doi: 10.1016/j.ensm.2017.07.006
- Han, F., Yue, J., Fan, X., Gao, T., Luo, C., Ma, Z., et al. (2016). High-performance all-solid-state lithium-sulfur battery enabled by a mixed-conductive Li_2S nanocomposite. *Nano Lett.* 16, 4521–4527. doi: 10.1021/acs.nanolett.6b01754
- Hart, N., Shi, J., Zhang, J., Fu, C., and Guo, J. (2018). Lithium sulfide-carbon composites via aerosol spray pyrolysis as cathode materials for lithium-sulfur batteries. *Front. Chem.* 6:674. doi: 10.3389/fchem.2018.00476
- Jeong, S., Bresser, D., Buchholz, D., Winter, M., and Passerini, S. (2013). Carbon coated lithium sulfide particles for lithium battery cathodes. *J. Power Sources* 235, 220–225. doi: 10.1016/j.jpowsour.2013.01.084
- Jha, H., Buchberger, I., Cui, X., Meini, S., and Gasteiger, H. A. (2015). Li-S batteries with Li_2S cathodes and Si/C anodes. *J. Electrochem. Soc.* 162, A1829–A1835. doi: 10.1149/2.0681509jes
- Jung, Y., and Kang, B. (2016). Understanding abnormal potential behaviors at the 1st charge in Li_2S cathode material for rechargeable Li-S batteries. *Phys. Chem. Chem. Phys.* 18:21500. doi: 10.1039/C6CP03146C
- Kohl, M., Bruckner, J., Bauer, I., Althues, H., and Kaskel, S. (2015). Synthesis of highly electrochemically active Li_2S nanoparticles for lithium-sulfur-batteries. *J. Mater. Chem. A* 3, 16307–16312. doi: 10.1039/C5TA04504E
- Lee, S., Lee, Y. J., and Sun, Y. (2016). Nanostructured lithium sulfide materials for lithium-sulfur batteries. *J. Power Sources* 323, 174–188. doi: 10.1016/j.jpowsour.2016.05.037
- Li, Z., Zhang, S., Zhang, C., Ueno, K., Yasuda, T., Tatara, R., et al. (2015). One-pot pyrolysis of lithium sulfate and graphene nanoplatelet aggregates: *in situ* formed Li_2S /graphene composite for lithium-sulfur batteries. *Nanoscale* 7, 14385–14392. doi: 10.1039/C5NR03201F
- Liang, S., Liang, C., Xia, Y., Xu, H., Huang, H., Tao, X., et al. (2016). Facile synthesis of porous $\text{Li}_2\text{S}@C$ composites as cathode materials for lithium-sulfur batteries. *J. Power Sources* 306, 200–207. doi: 10.1016/j.jpowsour.2015.12.030
- Liu, J., Nara, H., Yokoshima, T., Momma, T., and Osaka, T. (2015a). Li_2S cathode modified with polyvinylpyrrolidone and mechanical milling with carbon. *J. Power Sources* 273, 1136–1141. doi: 10.1016/j.jpowsour.2014.09.179
- Liu, J., Nara, H., Yokoshima, T., Momma, T., and Osaka, T. (2015b). Micro-scale $\text{Li}_2\text{S-C}$ composite preparation from Li_2SO_4 for cathode of lithium ion battery. *Electrochim. Acta* 183, 70–77. doi: 10.1016/j.electacta.2015.07.116
- Lv, D., Zheng, J., Li, Q., Xie, X., Ferrara, S., Nie, Z., et al. (2015). High energy density lithium-sulfur batteries: challenges of thick sulfur cathodes. *Adv. Energy Mater.* 5:1402290. doi: 10.1002/aenm.201402290

- Ma, L., Hendrickson, K. E., Wei, S., and Archer, L. A. (2015). Nanomaterials: science and applications in the lithium-sulfur battery. *Nano Today* 10, 315–338. doi: 10.1016/j.nantod.2015.04.011
- Manthiram, A., Chung, S. H., and Zu, C. (2015). Lithium-sulfur batteries: progress and prospects. *Adv. Mater.* 27, 1980–2006. doi: 10.1002/adma.201405115
- Peng, H., Huang, J., Cheng, X., and Zhang, Q. (2017). Review on high-loading and high-energy lithium-sulfur batteries. *Adv. Energy Mater.* 7:1700260. doi: 10.1002/aenm.201700260
- Seh, Z. W., Wang, H., Hsu, P., Zhang, Q., Li, W., Zheng, G., et al. (2014). Facile synthesis of Li₂S-polypyrrole composite structures for high-performance Li₂S cathodes. *Energy Environ. Sci.* 7, 672–676. doi: 10.1039/c3ee43395a
- Tan, G., Xu, R., Xing, Z., Yuan, Y., Lu, J., Wen, J., et al. (2017). Burning lithium in CS₂ for high-performing compact Li₂S-graphene nanocapsules for Li-S batteries. *Nat. Energy.* 2:17090. doi: 10.1038/nenergy.2017.90
- Vizintin, A., Chabanne, L., Tchernychova, E., Arcon, I., Stievano, L., Aquilanti, G., et al. (2017). The mechanism of Li₂S activation in lithium-sulfur batteries: can we avoid the polysulfide formation? *J. Power Sources* 344, 208–217. doi: 10.1016/j.jpowsour.2017.01.112
- Wang, C., Wang, X., Yang, Y., Kushima, A., Chen, J., Huang, Y., et al. (2015). Slurryless Li₂S/reduced graphene oxide cathode paper for high-performance lithium sulfur battery. *Nano Lett.* 15, 1796–1802. doi: 10.1021/acs.nanolett.5b00112
- Wang, D., Xie, D., Yang, T., Zhang, Y., Wang, X., Xia, X., et al. (2016). Conversion from Li₂SO₄ to Li₂S@C on carbon paper matrix: a novel integrated cathode for lithium-sulfur batteries. *J. Power Sources* 331, 475–480. doi: 10.1016/j.jpowsour.2016.09.033
- Wild, M., O'Neill, L., Zhang, T., Purkayastha, R., Minton, G., Marinescu, M., et al. (2015). Lithium sulfur batteries, a mechanistic review. *Energy Environ. Sci.* 8:3477. doi: 10.1039/C5EE01388G
- Wu, F., Kim, H., Magasinski, A., Lee, J., Lin, H., and Yushin, G. (2014a). Harnessing steric separation of freshly nucleated Li₂S nanoparticles for bottom-up assembly of high-performance cathodes for lithium-sulfur and lithium-ion batteries. *Adv. Energy Mater.* 4:1400196. doi: 10.1002/aenm.201400196
- Wu, F., Lee, J., Magasinski, A., Kim, H., and Yushin, G. (2014b). Solution-based processing of graphene-Li₂S composite cathodes for lithium-ion and lithium-sulfur batteries. *Part. Part. Syst. Charact.* 31, 639–644. doi: 10.1002/ppsc.201300358
- Wu, F., Lee, J. T., Fan, F., Nitta, N., Kim, H., Zhu, J., et al. (2015). A hierarchical particle-shell architecture for long-term cycle stability of Li₂S cathodes. *Adv. Mater.* 27, 5579–5586. doi: 10.1002/adma.201502289
- Wu, F., Lee, J. T., Zhao, E., Zhang, B., and Yushin, G. (2016). Graphene-Li₂S-carbon nanocomposite for lithium-sulfur batteries. *ACS Nano* 10, 1333–1340. doi: 10.1021/acsnano.5b06716
- Wu, F., Magasinski, A., and Yushin, G. (2014c). Nanoporous Li₂S and MWCNT-linked Li₂S powder cathodes for lithium-sulfur and lithium-ion battery chemistries. *J. Mater. Chem. A* 2, 6064–6070. doi: 10.1039/C3TA14161F
- Yang, Y., McDowell, M. T., Jackson, A., Cha, J. J., Hong, S. S., and Cui, Y. (2010). New nanostructured Li₂S/silicon rechargeable battery with high specific energy. *Nano Lett.* 10, 1486–1491. doi: 10.1021/nl100504q
- Yang, Y., Zheng, G., Misra, S., Nelson, J., Toney, M. F., and Cui, Y. (2012). High-capacity micrometer-sized Li₂S particles as cathode materials for advanced rechargeable lithium-ion batteries. *J. Am. Chem. Soc.* 134, 15387–15394. doi: 10.1021/ja3052206
- Yang, Z., Guo, J., Das, K. S., Yu, Y., Zhou, Z., Abruna, D. H., et al. (2013). *In situ* synthesis of lithium sulfide-carbon composites as cathode materials for rechargeable lithium batteries. *J. Mater. Chem. A* 1, 1433–1440. doi: 10.1039/C2TA00779G
- Ye, F., Noh, H., Lee, J., Lee, H., and Kim, H. (2018). Li₂S/carbon nanocomposite strips from a low-temperature conversion of Li₂SO₄ as high-performance lithium-sulfur cathodes. *J. Mater. Chem. A* 6, 6617–6624. doi: 10.1039/C8TA00515J
- Yu, M., Wang, Z., Wang, Y., Dong, Y., and Qiu, J. (2017). Freestanding flexible Li₂S paper electrode with high mass and capacity loading for high-energy Li-S batteries. *Adv. Energy Mater.* 7:1700018. doi: 10.1002/aenm.201700018
- Zhang, J., Shi, Y., Ding, Y., Peng, L., Zhang, W., and Yu, G. (2017). A conductive molecular framework derived Li₂S/N, P-codoped carbon cathode for advanced lithium-sulfur batteries. *Adv. Energy Mater.* 7:1602876. doi: 10.1002/aenm.201602876
- Zheng, S., Li, X., Yan, B., Hu, Q., Xu, Y., Xiao, X., et al. (2017). Transition-metal (Fe, Co, Ni) based metal-organic frameworks for electrochemical energy storage. *Adv. Energy Mater.* 7:1602733. doi: 10.1002/aenm.201602733
- Zhou, G., Paek, E., Hwang, G. S., and Manthiram, A. (2016). High-performance lithium-sulfur batteries with a self-supported, 3D Li₂S-doped graphene aerogel cathodes. *Adv. Energy Mater.* 6:1501355. doi: 10.1002/aenm.201501355

Conflict of Interest Statement: The authors declare that the research was conducted in the absence of any commercial or financial relationships that could be construed as a potential conflict of interest.

Copyright © 2019 Shi, Zhang, Zhao, Yan, Hart and Guo. This is an open-access article distributed under the terms of the Creative Commons Attribution License (CC BY). The use, distribution or reproduction in other forums is permitted, provided the original author(s) and the copyright owner(s) are credited and that the original publication in this journal is cited, in accordance with accepted academic practice. No use, distribution or reproduction is permitted which does not comply with these terms.